Talanta 89 (2012) 317–321

Contents lists available at SciVerse ScienceDirect

Talanta

journal homepage: www.elsevier.com/locate/talanta

Label-free, sensitive detection of Hg(II) with gold nanoparticles by using dynamic light scattering technique

Cen Xiong, Liansheng Ling*

School of Chemistry And Chemical Engineering, Sun Yat-Sen University, Guangzhou, Guangdong 510275, PR China

ARTICLE INFO

Article history:
Received 5 October 2011
Received in revised form 5 December 2011
Accepted 5 December 2011
Available online 19 December 2011

Keywords:
Mercury ion
Dynamic light scattering
Oligonucleotide
Gold nanoparticles

ABSTRACT

A label-free method for sensitive detection of Hg^{2+} was developed with gold nanoparticles (AuNPs) by using dynamic light scattering (DLS) technique. Oligonucleotide 5′-TTT CTT CTT CGT TGT TGT TT-3′ could transform from uncoil to rigid duplex or hairpin structure upon addition of Hg^{2+} ions, which was confirmed by experiments of fluorescence resonance energy transfer and change of melting temperature. The change of DNA structure reduced its adsorption ability on the surface of AuNPs, and resulted in the aggregation of AuNPs in the salt solution, which could be estimated with average hydrodynamic diameter by using DLS technique. Under the optimum conditions, the average diameter increased linearly with the concentration of Hg^{2+} over the range from 0.75 nM to 25 nM, the linear regression equation was $D = 46.7 + 2.0\,C$ (nM, $R = 0.9958$), with a detection limit of 0.43 nM.

1. Introduction

Mercury(II) ion is existed widely in environment, which can cause long-term damage to biological systems and bring oxidative damage to human body [1]. Therefore, many efforts were dedicated to develop sensitive method for detection of mercury(II) ion. Traditional method such as inductively coupled plasma mass spectrometry (ICP–MS) and inductively coupled plasma atomic emission spectrometry (ICP-AES) has been applied in the detection of Hg^{2+} successfully [2,3]. Since Ono and co-workers reported the specific binding property of Hg^{2+} with T–T mismatched base pairs, plenty of DNA-based fluorescent sensors for Hg^{2+} were constructed by use of the formation of T–Hg^{2+}–T coordination [4–8].

Color of gold nanoparticles (AuNPs) depend on space of interparticle, and disperse state of oligonucleotide modified AuNPs can be controlled by the DNA hybridization [9–12]. Therefore, a series of colorimetric sensors for Hg^{2+} were developed with oligonucleotide functionalized AuNPs based upon their specific binding property with T–T mismatched base pair, the minimum detection limit of these methods was 100 nM [13,14]. On the other hand, several label-free sensors for Hg^{2+} were constructed with unmodified AuNPs based upon the adsorption ability of oligonucleotide on the surface of AuNPs changed with the concentration of Hg^{2+} [15–22].

Dynamic light scattering (DLS), which could be used to detect the average hydrodynamic diameter change of nanoparticles [23], was applied to characterize the morphology of DNA conjugated AuNPs and study the DNA hybridization on the surface of AuNPs [24,25]. Due to the high sensitivity of the DLS technique, Huo et al. built bioassay for detection of target ssDNA and proteins successfully [26–28]. Moreover, this technique has been applied to analyse the cancer biomarker [29], gene fragment [7], lead ions [30,31], arsenic [32], TNT [33], and dsDNA [34] by coupling with the gold nanoparticles. Here we established a DLS sensor for mercury (II) ion with unmodified AuNPs by transducing the Hg^{2+} – induced DNA hybridization into the signal change of average hydrodynamic diameter.

2. Experimental

2.1. Reagents

Oligonucleotides were synthesized by Sangon Co. (Shanghai, China) and used without further purification. $HAuCl_4{\cdot}3H_2O$ (Sigma–Aldrich Co.), $HgCl_2$ (Sigma–Aldrich Co.), 2-[4-(2-hydroxyethyl)-1-piperazinyl]ethanesulfonic acid (HEPES) were analytical reagent grade. Nanopure water (18.1 MΩ) was obtained from a 350 Nanopure water system (Guangzhou Crystalline Resdurce Desalination of Sea Water and Treatment Co. Ltd.) and was used for the research.

2.2. Instrumentation

Average hydrodynamic diameter was measured by using Zetaplus/90plus Dynamic Light Scattering Instrument (Brookhaven

* Corresponding author. Tel.: +86 20 84110156.
E-mail address: cesllsh@mail.sysu.edu.cn (L. Ling).

0039-9140/$ – see front matter © 2011 Elsevier B.V. All rights reserved.
doi:10.1016/j.talanta.2011.12.036

Instrument Co., USA). The DLS instrument was operated under the following conditions: the temperature was 25 °C, the detector angle was 90o, the incident laser wavelength was 683 nm and the laser power was 100 mW, respectively. The sizes distribution was obtained by using non-negative least squares (NNLS) analysis method (intensity average). A TU-1901 UV-visible absorption spectrometer was used to obtain the absorption spectrum and draw up the melting curve. The size distributions of the nanoparticles were learned from the transmission electron microscope (TEM) images, which were recorded with a JEM-2010HR transmission electron microscope (Japan).

2.3. Design of oligonucleotide sequence

Oligonucleotide 5′-TTT CTT CTT CGT TGT TGT TT-3′ (Oligo-1) was designed for DLS research. Oligonucleotide 5′-FAM-TTT CTT CTT CGT TGT TGT TT-3′ (Oligo-2) and Oligonucleotide 5′-TTTCTT CTT CGT TGT TGT TT-DABCYL-3′ (Oligo-3) were designed for investigating structure change of Oligo-1 upon addition of Hg^{2+}. Oligonucleotide 5′-CCA ACC CCC CAG AAA GAA TA-3′ (Oligo-4) was designed as the control sequence.

2.4. Synthesis and characterization of gold nanoparticles

Gold nanoparticles were synthesized using 2.0 ml 38.8 mM sodium citrate to reduce the 20 ml 1.0 mM $HAuCl_4$ [35]. The average size of 14.6 ± 2 nm of the AuNPs was calculated from the TEM picture that containing at least 100 particles, it was smaller than 33.7 nm that obtained from the DLS technique, which might be explained that DLS measure the hydrodynamic radius while TEM providing a more precise measurement of the hard AuNPs core [36]. The concentration of AuNPs was estimated with UV–visible absorption spectrum based on an extinction coefficient of $2.6 \times 10^8\ M^{-1}\ cm^{-1}$ at 520 nm for ~13 nm particles.

2.5. General procedure of DLS measurements

Generally, 40 μl 1.2 μM Oligo-1 solution was mixed with 60 μl HEPES buffer (10 mM, pH 7.5) solution including different concentrations of Hg^{2+} and incubated for 15 min. After that, 100 μl prepared AuNPs solution was added into this mixture to incubate for another 20 min, and then several microliter of salt solution (NaCl, final 0.06 M) was added. The DLS measurement was performed in 10 min. ICP–MS measurement was performed on a Thermo X Series II ICP/MS (Thermo Fisher Scientific Inc.)

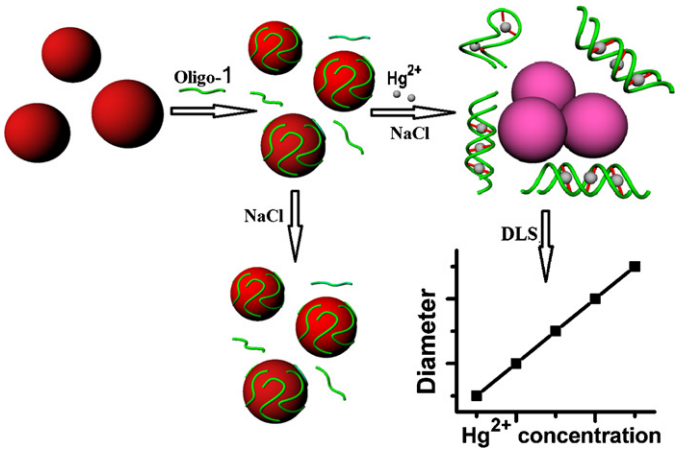

Fig. 1. The principle of biosensors for Hg^{2+} detection measured by DLS.

2.6. Fluorescence measurements

The fluorescence was measured by using an RF-5301PC spectrofluorimeter (Shimadzu, Japan) with IR sensitive detector. The fluorescence intensity was obtained from the emission spectrum at the wavelength of 610 nm. The slit width was 10 nm for excitation spectrum and 10 nm for emission spectrum respectively.

2.7. Melting temperature measurements

The TU-1901 UV-visible absorption spectrometer was used to obtain the absorption spectrum and draw up the melting curve.

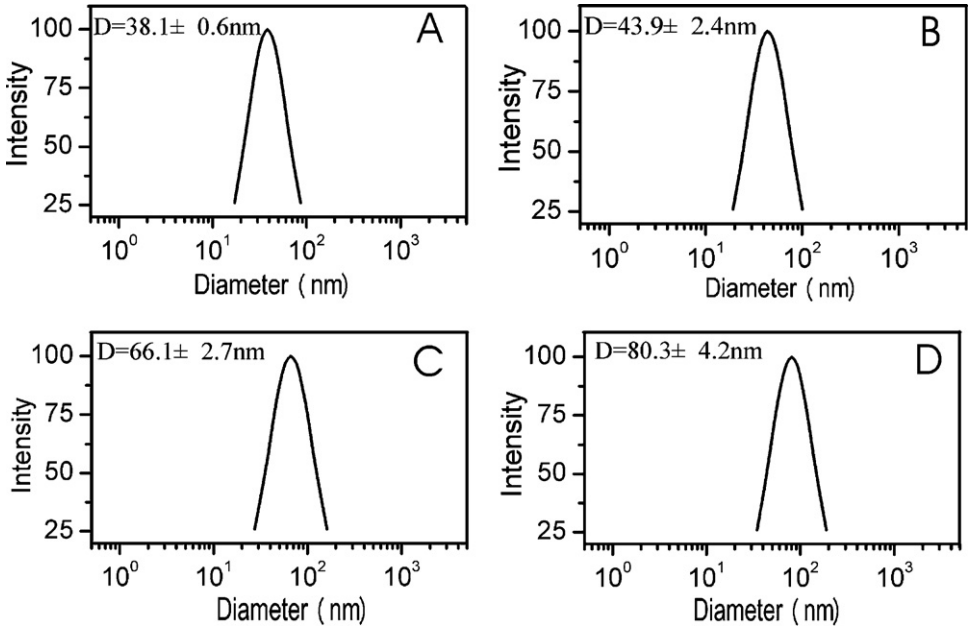

Fig. 2. The size distribution of Oligo-1 adsorbed AuNPs under different conditions. (A) 240 nM Oligo-1 + 5.75 nM AuNPs + 10 mM HEPES buffer (pH 7.5); (B) A + 0.06 M NaCl; (C) B + 10 nM Hg^{2+}; (D) B + 20 nM Hg^{2+}.

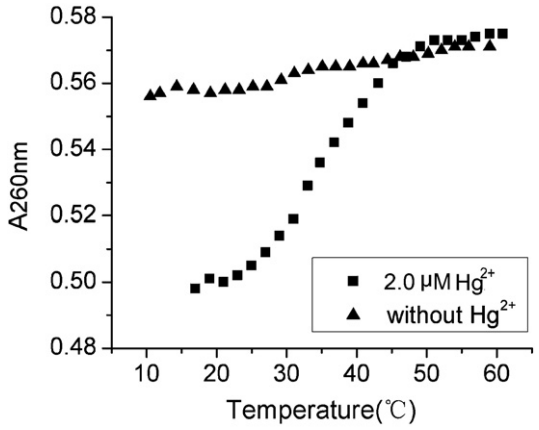

Fig. 3. The melting curves of 2.47 μM oligo-1 in the absence (curve *a*) and presence (curve *b*) of 2.0 μM Hg^{2+}. Experiments were performed in the HEPES buffer (10 mM, pH 7.5) containing 0.1 M NaCl.

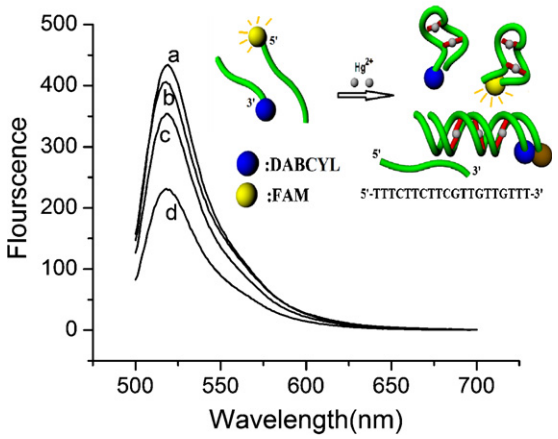

Fig. 4. Fluorescence spectra and the hybridization scheme of solutions of 50 nM FAM-Oligo-1 under different conditions. Curve *a*: 50 nM Oligo-2; Curve *b*: *a* + 16.0 nM Hg^{2+}; Curve *c*: *a* + 50 nM Oligo-3; Curve *d*: *c* + 16.0 nM Hg^{2+}. The hybridization was performed in HEPES buffer (10 mM, pH 7.5) containing 0.06 M NaCl, and measured after 1.5 h of incubation time.

3. Results and discussion

3.1. Principle of the DLS method of Hg^{2+} detection

The principle of the sensor for Hg^{2+} was demonstrated in Fig. 1, oligonucleotide 5′-TTT CTT CTT CGT TGT TGT TT-3′ (Oligo-1) was designed for the research, it could adsorb on the surface of AuNPs and protect AuNPs from aggregation. Upon addition of Hg^{2+}, DNA hybridization occurred between Oligo-1 strands because of the formation of T–Hg^{2+}–T bond, resulted in the desorption of Oligo-1 from the surface of AuNPs, accompany with the aggregation of AuNPs in the presence of NaCl. These changes could be estimated with the average diameter of AuNPs by using dynamic light scattering technique.

Fig. 2 demonstrated the average hydrodynamic diameter of Oligo-1 adsorbed AuNPs under different conditions. The average diameter of Oligo-1 adsorbed AuNPs was 38.1 nm (the bare AuNPs was about 33.7 nm, data not shown), and it increased to 43.9 nm in the presence of 0.06 M NaCl, which might be attributed to the slight aggregation of small amount of unprotected AuNPs. Furthermore, the average diameter increased from 43.9 nm to 66.1 and 80.3 nm upon addition of 10 nM Hg^{2+} and 20 nM Hg^{2+}, respectively. These might be due to the change of DNA structure upon addition of Hg^{2+} [4]. To investigate the possible change of Oligo-1 upon addition of Hg^{2+}, the melting curve of Oligo-1 before and after the addition of Hg^{2+} were studied. As shown in Fig. 3, there was no manifest melting temperature could be found from the melting curve of Oligo-1, which meant that the structure of Oligo-1 kept stable when the temperature increased from 10 °C to 55 °C. While a melting temperature of 45 °C could be observed from the melting curve of Oligo-1 in the presence of Hg^{2+}, which meant that the structure of Oligo-1 changed upon addition of Hg^{2+}.

3.2. The DNA structure transformation induced by mercury ions

To further explore the structure change of Oligo-1 upon addition of Hg^{2+}, FAM was modified at the 5′ end of Oligo-1 (Oligo-2) to act as donor, DABCYL modified Oligo-1 (Oligo-3) was designed as acceptor. The fluorescent spectra of Oligo-2 under different conditions were shown in Fig. 4, Oligo-2 emitted strong fluorescence, little change was occurred upon addition of Hg^{2+} (curve $a \rightarrow b$). However, the fluorescence of Oligo-2 decreased slightly when Oligo-3 was added (curve *c*). Moreover, it was quenched dramatically upon addition of Oligo-3 together with Hg^{2+} (curve *d*), which revealed that DNA hybridization occurred between Oligo-2 and Oligo-3 upon addition of Hg^{2+}. It was interesting that the fluorescence quenching efficiency was only 50%, which was much lower than 80% that reported previously [5]. These results indicated that most of Oligo-1 formed duplex DNA upon addition of Hg^{2+}, only small part of Oligo-1 strands formed hairpin structure, which had nothing to do with the fluorescence quenching. Therefore, the change of average diameter of Oligo-1 adsorbed AuNPs induced by Hg^{2+} could be explained as following: single – stranded Oligo-1 could adsorb on the surface of AuNPs and protect the AuNPs from aggregation in the presence of NaCl, while the Oligo-1 formed rigid dsDNA or hairpin structure upon addition of Hg^{2+}, which induced the desorption of Oligo-1 from the surface of AuNPs and could not protect the AuNPs from aggregation in the presence of NaCl, resulted in the increase of the average diameter of Oligo-1 adsorbed AuNPs.

3.3. Optimization of the experimental conditions

To optimize the experimental conditions, the differential of average hydrodynamic diameter (ΔD) was used to estimate the signal change, which could be defined as $\Delta D = D_{Hg2+} - D_{no\ Hg2+}$ (here D_{Hg2+} denotes the average diameter of Oligo-1 adsorbed AuNPs in the presence of Hg^{2+}, and $D_{no\ Hg2+}$ represents the average diameter of Oligo-1 adsorbed AuNPs in the absence of Hg^{2+}). The disperse state of AuNPs depends on the amount of DNA that adsorbed on the surface, so the effect of the concentration of Oligo-1 on ΔD was investigated over the range from 50 nM to 360 nM. As shown in Fig. 5A, the value of ΔD increased gradually with the concentration of Oligo-1 over the range of 50–240 nM, and then declined with further increase of the Oligo-1. These results meant that suitable concentration of Oligo-1 was necessary for measurement, too low and too high concentration of Oligo-1 were both unfavorable for the signal of ΔD. Thereby 240 nM Oligo-1 was selected for the research. Chloride sodium can affect the disperse state of AuNPs, and the effect of the concentration of NaCl on the ΔD was investigated over the range from 0.025 M to 0.08 M. As shown in Fig. 5B, the ΔD increased sharply with the concentration of NaCl over the range of 0.025–0.04 M, and then it increased slightly when the concentration varied within the range of 0.04–0.08 M. Therefore, 0.06 M was chosen in this work. DNA hybridization and the state of Hg^{2+} depends on the pH value of environment, so the disperse state of Oligo-1 adsorbed AuNPs might be affected by pH value, and the effect of pH value on the ΔD was studied during the pH range of 6.5–8.5. As shown in Fig. 5C, the ΔD increased with the pH value over the range from 6.5 to 7.5, then it declined with the increase of pH value over the range of 7.5–8.5, so pH 7.5 was used for

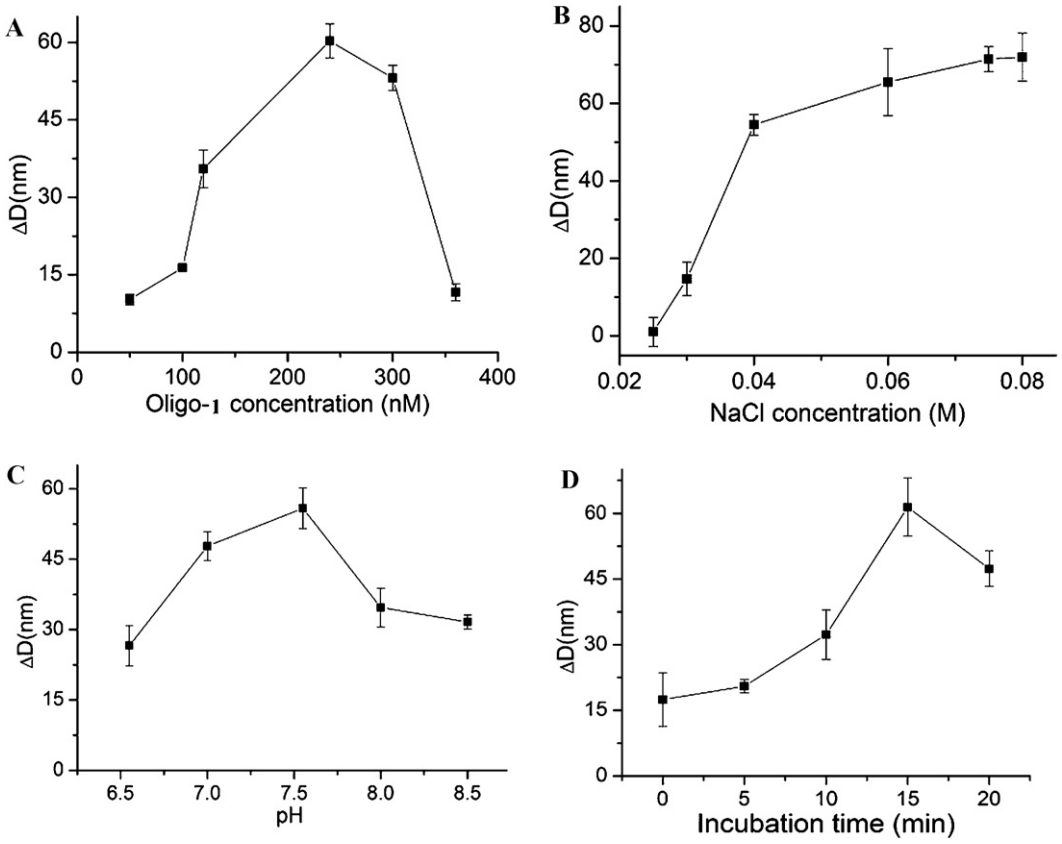

Fig. 5. (A) The effect of Oligo-1 concentration on the difference of diameter (ΔD); (B) the effect of NaCl concentration on the ΔD; (C) the effect of pH on the ΔD; (D) the effect of incubation time on the ΔD prior to the addition of NaCl. (A) AuNPs: 5.75 nM, NaCl: 0.06 M, Hg^{2+}: 50 nM, pH: 7.5; (B) AuNPs: 5.75 nM, Oligo-1: 240 nM, Hg^{2+}: 50 nM, pH: 7.5; (C) AuNPs: 5.75 nM, Oligo-1: 40 nM, NaCl: 0.06 M, Hg^{2+}: 50 nM; (D) AuNPs: 5.75 nM, Oligo-1: 240 nM, NaCl: 0.06 M, Hg^{2+}: 50 nM, pH: 7.5.

Table 1
Determination of Hg^{2+} in water samples with the proposed method and ICP–MS.

Samples	Added nM	Found by proposed method nM	RSD (n = 6,%)	Recovery (n = 6,%)	Found by ICP–MS nM
Nano pure water	0	Not found	–	–	Not found
	2.50	2.39	1.7	95.6	2.46
	6.00	5.87	2.6	97.8	5.60
	12.0	12.0	3.9	100.2	11.1
River water	0	Not found	–	–	0.36
	2.50	2.42	3.1	96.8	2.32
	6.00	5.86	3.7	95.0	5.70
	12.0	11.5	4.0	97.5	11.7
Pond water 1	0	Not found	–	–	0.39
	2.50	2.40	3.4	96.1	2.54
	6.00	5.73	4.5	95.5	6.20
	12.0	11.7	3.8	97.3	12.8
Pond water 2	0	Not found	–	–	0.29
	2.50	2.62	4.1	104.8	2.59
	6.00	6.30	5.2	105.0	5.80
	12.0	12.6	4.6	104.9	11.5

the research. The incubation time might affect the DNA hybridization based upon the formation of T–Hg^{2+}–T coordination, and the adsorption ability of Oligo-1 was affected as well. Hence the effect of incubation time on the ΔD was investigated over the time range of 0–20 min. As shown in Fig. 5D, 15 min was the optimum incubation time, and accordingly 15 min of incubation was used throughout the research.

3.4. Sensitivity and selectivity

Under the conditions of 240 nM Oligo-1, 5.75 nM AuNPs, 10 mM HEPES buffer (pH 7.5) and 0.06 M NaCl, the average hydrodynamic diameter of the solution of Oligo-1 adsorbed AuNPs was proportional to the concentration of Hg^{2+} over the range from 0.75 nM to 25 nM, as shown in Fig. 6A, the linear regression equation was $D = 46.7 + 2.0\,C$ (nM, $R = 0.9958$), with a detection limit of 0.43 nM (DL = 3δ/slope). This detection limit was quite lower than the safety level of drinking water (10 nM Hg^{2+}) that permitted by US Environmental Protection Agency. To explore the selectivity of this method, the response from a number of environmental – related metals ions such as Ca^{2+}, Co^{2+}, Cr^{2+}, Pb^{2+}, Cu^{2+}, K^{+}, Ba^{2+}, Cd^{2+}, Al^{3+}, Zn^{2+} and Hg^{2+} was investigated. As shown in Fig. 6B, compared to that of blank solution, the addition of 50 nM Hg^{2+} resulted in an obvious increase of average diameter. On the contrary, little change could

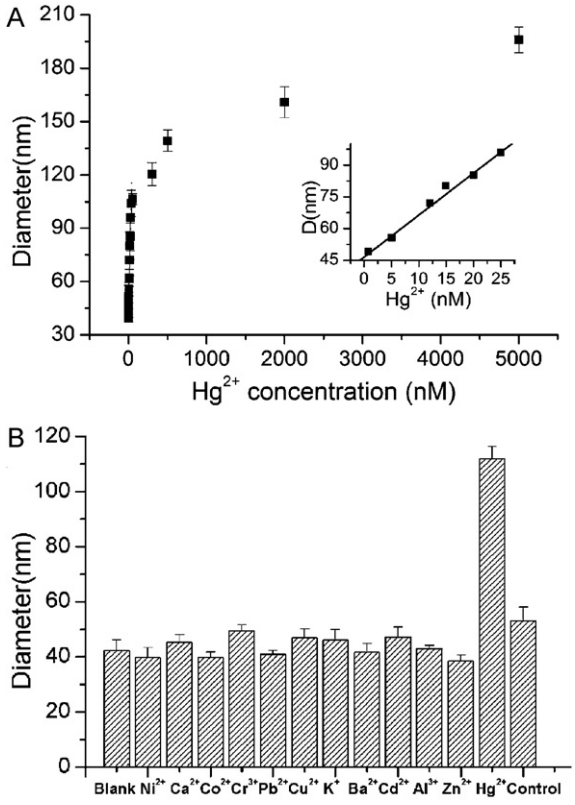

Fig. 6. (A) Plots of diameters of AuNPs versus different concentration of Hg^{2+}. The inset shows the calibration curve for Hg^{2+}. (B) Selectivity of the method. Experimental conditions: Oligo-1 (240 nM), AuNPs (5.75 nM), NaCl (0.06 M). For the ion selectivity, the concentration of Hg^{2+} was 50 nM, while other metal ions were 2.0 μM respectively. The control experiment was performed with Oligo-2 (240 nM) and 500 nM Hg^{2+}.

be observed upon addition of other metal ion with a concentration of 2.0 μM. Moreover, a control experiment was carried out by replacing the Oligo-1 with Oligo-4 (control), the average diameter was almost the same with that of blank. These results indicated the good selectivity of the assay.

3.5. Application

To explore the feasibility of the assay, it was applied to detect the concentration of Hg^{2+} in three water samples. The water samples were obtained from the ZhuJiang river and two ponds in our campus. The samples were first filtered through a 0.22 μm membrane to remove the suspended solids [19]. The results were summarized in Table 1, No Hg^{2+} was found from the water samples, the addition and recovery experiments were carried out to test feasibility of the assay. The recoveries varied in the range from 95.0% to 104.9% when 2.5 nM, 6.0 nM, 12.0 nM of Hg^{2+} was added respectively, and the RSD values varied in the range of 1.7–5.2%. Moreover, results that obtained from the proposed method were in good agreement with that obtained from the method of ICP–MS (inductively coupled plasma mass spectrometry). These results suggested that the method was practical and reliable.

4. Conclusions

In summary, a sensitive DLS assay for detection of Hg^{2+} was established with unmodified AuNPs and Oligonucleotide. Hg^{2+} ions could induce the conformation of Oligo-1 changed from single-strand structure to duplex or hairpin structure through the formation of T–Hg^{2+}–T coordination, it triggered the change of adsorption ability of Oligo-1 on the surface of AuNPs, accompany with the change of the NaCl resistance of AuNPs, which could be estimated with the average hydrodynamic diameter of AuNPs by using DLS technique. Therefore, the average diameter of Oligo-1 adsorbed AuNPs depended on the concentration of Hg^{2+}, and the average diameter was proportional to the concentration of Hg^{2+} over the range from 0.75 nM to 25 nM, with a detection limit of 0.43 nM. Moreover, the assay could be extended to developing other sensors based upon the change of DNA conformation.

Acknowledgment

This work was supported by the National Natural Science Foundation of China (No. 20975116).

References

[1] M.R. Knecht, M. Sethi, Anal. Bioanal. Chem. 394 (2009) 33–46.
[2] D.R. Wiederin, F.G. Smith, R.S. Houk, Anal. Chem. 63 (1991) 219–225.
[3] B.W. Acon, J.A. McLean, A. Montaser, Anal. Chem. 72 (2000) 1885–1893.
[4] Y. Miyake, H. Togashi, M. Tashiro, H. Yamaguchi, S. Oda, M. Kudo, Y. Tanaka, Y. Kondo, R. Sawa, T. Fujimoto, T. Machinami, A. Ono, J. Am. Chem. Soc. 128 (2006) 2172–2173.
[5] Y.W. Lin, H.T. Ho, C.C. Huang, H.T. Chang, Nucl. Acids Res. 19 (2008) e123.
[6] R. Yang, J. Jin, L. Long, Y. Wang, H. Wang, W. Tan, Chem. Commun. (2008) 322–324.
[7] D. Gao, Z. Sheng, H. Han, Anal. Chim. Acta 696 (2011) 1–5.
[8] L. Guo, H. Hu, R. Sun, G. Chen, Talanta 79 (2009) 775–779.
[9] C.A. Mirkin, R.L. Letsinger, R.C. Mucic, J.J. Storhoff, Nature 382 (1996) 607–609.
[10] W.J. Parak, T. Pellegrino, C.M. Micheel, D. Gerion, S.C. Williams, A.P. Alivisatos, Nano Lett. 3 (2003) 33–36.
[11] T.A. Taton, C.A. Mirkin, R.L. Letsinger, Science 289 (2000) 1757–1760.
[12] N.L. Rosi, C.A. Mirkin, Chem. Rev. 105 (2005) 1547–1562.
[13] J.S. Lee, M.S. Han, C.A. Mirkin, Angew. Chem. Int. Ed. 46 (2007) 4093–4906.
[14] S. He, C. Zhu, S. Song, L. Wang, Y. Long, C. Fan, Chem. Commun. (2008) 4885–4887.
[15] D. Li, A. Wieckowska, I. Willner, Angew. Chem. 120 (2008) 3991–3995.
[16] C.W. Liu, Y.T. Hsieh, C.C. Huang, Z.H. Lin, H.T. Chang, Chem. Commun. (2008) 2242–2244.
[17] Y. Wang, F. Yang, X. Yang, Biosens. Bioelectron. 25 (2010) 1994–1998.
[18] X. Xu, J. Wang, K. Jiao, X. Yang, Biosens. Bioelectron. 24 (2009) 3153–3158.
[19] Z.D. Liu, Y.F. Li, J. Ling, C.Z. Huang, Environ. Sci. Technol. 43 (2009) 5022–5027.
[20] Y. Wang, F. Yang, X. Yang, ACS Appl. Mater. Interface 2 (2010) 339–342.
[21] Z. Jiang, Y. Fan, M. Chen, A. Liang, X. Liao, G. Wen, X. Shen, X. He, H. Pan, H. Jiang, Anal. Chem. 81 (2009) 5439–5445.
[22] X. Zuo, H. Wu, J. Toh, S.F.Y. Li, Talanta 82 (2010) 1642–1646.
[23] H. Jans, X. Liu, L. Austin, G. Maes, Q. Huo, Anal. Chem. 81 (2009) 9425–9432.
[24] J. Xu, S.L. Craig, Langmuir 23 (2007) 2015–2020.
[25] W. Zhao, W. Chiuman, J.C.F. Lam, S.A. McManus, W. Chen, Y. Cui, R. Pelton, M.A. Brook, Y. Li, J. Am. Chem. Soc. 130 (2008) 3610–3618.
[26] Q. Dai, X. Liu, J. Coutts, L. Austin, Q. Huo, J. Am. Chem. Soc. 130 (2008) 8138–8139.
[27] X. Liu, Q. Huo, J. Immunol. Methods 349 (2009) 38–44.
[28] J. Bogdanovic, J. Colon, C. Baker, Q. Huo, Anal. Biochem. 405 (2010) 96–102.
[29] X. Liu, Q. Dai, L. Austin, J. Coutts, G. Knowles, J. Zou, H. Chen, Q. Huo, J. Am. Chem. Soc. 130 (2008) 2780–2782.
[30] X. Miao, L. Ling, X. Shuai, Chem. Commun. 47 (2011) 4192–4194.
[31] L. Beqa, A.K. Singh, S.A. Khan, D. Senapati, S.R. Arumugam, P.C. Ray, ACS Appl. Mater. Interface 3 (2011) 668–673.
[32] J.R. Kalluri, T. Arbneshi, S. Afrin Khan, A. Neely, P. Candice, B. Varisli, M. Washington, S. McAfee, B. Robinson, S. Banerjee, Angew. Chem. 121 (2009) 9848–9851.
[33] S.S.R. Dasary, D. Senapati, A.K. Singh, Y. Anjaneyulu, H. Yu, P.C. Ray, ACS Appl. Mater. Interfaces 2 (2010) 3455–3460.
[34] X.M. Miao, C. Xiong, W.W. Wang, L.S. Ling, X.T. Shuai, Chem. Eur. J. 17 (2011) 11230–11236.
[35] R. Jin, G. Wu, Z. Li, C.A. Mirkin, G.C. Schatz, J. Am. Chem. Soc. 125 (2003) 1643–1654.
[36] F.D. Sikkema, M. Comellas-Aragonès, R.G. Fokkink, B.J.M. Verduin, J.J.L.M. Cornelissen, R.J.M. Nolte, Org. Biomol. Chem. 5 (2007) 54–57.